

# Bacterial sulfur disproportionation constrains timing of Neoproterozoic oxygenation

Marcus Kunzmann<sup>1,2</sup>, Thi Hao Bui<sup>1</sup>, Peter W. Crockford<sup>1</sup>, Galen P. Halverson<sup>1</sup>, Clint Scott<sup>3</sup>, Timothy W. Lyons<sup>4</sup>, and Boswell A. Wing<sup>1,5</sup>

<sup>1</sup>Department of Earth and Planetary Sciences and Geotop, McGill University, 3450 University Street, Montreal, Quebec H3A 0E8, Canada

<sup>2</sup>CSIRO Mineral Resources, Australian Resources Research Centre, 26 Dick Perry Avenue, Kensington, WA 6151, Australia, and Northern Territory Geological Survey, Darwin, NT 0800, Australia

<sup>3</sup>U.S. Geological Survey, National Center, 12201 Sunrise Valley Drive, Reston, Virginia 20192, USA

<sup>4</sup>Department of Earth Sciences, University of California, Riverside, California 92521-0423, USA

<sup>5</sup>Department of Geological Sciences, University of Colorado Boulder, UCB 399, Boulder, Colorado 80309-0399, USA

## ABSTRACT

**Various geochemical records suggest that atmospheric O<sub>2</sub> increased in the Ediacaran (635–541 Ma), broadly coincident with the emergence and diversification of large animals and increasing marine ecosystem complexity. Furthermore, geochemical proxies indicate that seawater sulfate levels rose at this time too, which has been hypothesized to reflect increased sulfide oxidation in marine sediments caused by sediment mixing of the newly evolved macrofauna. However, the exact timing of oxygenation is not yet understood, and there are claims for significant oxygenation prior to the Ediacaran. Furthermore, recent evidence suggests that physical mixing of sediments did not become important until the late Silurian. Here we report a multiple sulfur isotope record from a ca. 835–630 Ma succession from Svalbard, further supported by data from Proterozoic strata in Canada, Australia, Russia, and the United States, in order to investigate the timing of oxygenation. We present isotopic evidence for onset of globally significant bacterial sulfur disproportionation and reoxidative sulfur cycling following the 635 Ma Marinoan glaciation. Widespread sulfide oxidation helps to explain the observed first-order increase in seawater sulfate concentration from the earliest Ediacaran to the Precambrian-Cambrian boundary by reducing the amount of sulfur buried as pyrite. Expansion of reoxidative sulfur cycling to a global scale also indicates increasing environmental O<sub>2</sub> levels. Thus, our data suggest that increasing atmospheric O<sub>2</sub> levels may have played a role in the emergence of the Ediacaran macrofauna and increasing marine ecosystem complexity.**

## INTRODUCTION

The evolution of atmospheric O<sub>2</sub> levels in the late Neoproterozoic is poorly understood, but the most recent studies indicate that the postulated Ediacaran rise in  $pO_2$  may have been less than previously thought (Sperling et al., 2015) and that the Ediacaran ocean may have largely remained anoxic, only marked by temporally restricted oxygenation events (Sahoo et al., 2016). However, the timing of oxygenation remains controversial because other studies propose significant pre-Ediacaran oxygenation (e.g., Blamey et al., 2016). This highlights that a detailed understanding of the timing of Neoproterozoic oxygenation is still required, which will in turn inform the temporal links and potential causal relationship between environmental change and early animal evolution. Considering the intimate links between the marine sulfur cycle and atmospheric O<sub>2</sub>, we established a multiple sulfur isotope record from ca. 835–630 Ma to test models for the timing of Neoproterozoic oxygenation.

In modern marine sediments, most of the H<sub>2</sub>S produced by microbial sulfate reduction (MSR) is reoxidized, either directly to sulfate or to intermediate S species (Jørgensen, 1990). Sulfate and intermediate S compounds such as S<sup>0</sup>, SO<sub>3</sub><sup>2-</sup>, and S<sub>2</sub>O<sub>3</sub><sup>2-</sup> are formed by reaction of H<sub>2</sub>S with O<sub>2</sub>, NO<sub>3</sub><sup>-</sup>, Fe(III), and Mn(IV) compounds (e.g., Elsgaard and Jørgensen, 1992), often mediated by chemolithotrophic sulfide-oxidizing bacteria (Aller and Rude, 1988; Canfield and Teske, 1996). Intermediate S species and sulfate can also form by oxidation of iron sulfide minerals with O<sub>2</sub>, NO<sub>3</sub><sup>-</sup> (biologically catalyzed), and Mn(IV) compounds (Schippers and Jørgensen, 2001, 2002). Some of the intermediate S species are further oxidized to sulfate or reduced again to sulfide. However, a significant proportion of intermediates are converted to H<sub>2</sub>S and SO<sub>4</sub><sup>2-</sup> by bacterial sulfur disproportionation (BSD; Jørgensen, 1990; Thamdrup et al., 1993), a metabolism that does not require an electron acceptor or donor. This step completes the reoxidative S

cycle, defined as the progression from sulfate reduction to sulfide oxidation and disproportionation of intermediate S compounds.

The transition from local reoxidative S cycling to a globally operating reoxidative S cycle in Earth's history requires enhanced oxidation of sulfide in marine sediments worldwide. Although Fe(III) and Mn(IV) may have been the most important oxidants for sulfide in marine sediments underlying the dominantly anoxic Proterozoic oceans, enhanced sulfide oxidation pathways ultimately require enhanced O<sub>2</sub> consumption, regardless of the type of proximal electron acceptor in the initial oxidative process. Enhanced biologically catalyzed production of S intermediates may additionally require an evolutionary radiation of nonphotosynthetic sulfide-oxidizing bacteria, previously proposed to be a direct consequence of increasing O<sub>2</sub> levels (Canfield and Teske, 1996). Therefore, onset of a globally operating reoxidative S cycle, identified by expansion of BSD in global marine sediments, is tantamount to evidence for increasing atmospheric O<sub>2</sub>. Identifying a switch from local to globally significant reoxidative S cycling thus presents an opportunity to better understand the timing of Neoproterozoic oxygenation.

BSD produces a negative <sup>34</sup>S-<sup>32</sup>S isotope fractionation in the sulfide products (Canfield et al., 1998) such that repeated cycles of sulfide oxidation and BSD may produce sedimentary sulfides that are isotopically lighter than those produced by MSR alone. However, MSR alone may cause maximum S isotope fractionations between sulfide and sulfate of as much as ~-70‰ (Canfield et al., 2010; Sim et al., 2011; Wing and Halevy, 2014). Because the  $\delta^{34}\text{S}$  values of pyrite in the geological record are typically <70‰ lighter than coeval seawater sulfate, it is difficult to identify BSD and a fingerprint of reoxidative sulfur cycling based on  $\delta^{34}\text{S}$  values in ancient environments alone. However, MSR and BSD can be distinguished

by measuring  $^{33}\text{S}$  in addition to  $^{32}\text{S}$  and  $^{34}\text{S}$  because each metabolism produces a distinctive  $\delta^{34}\text{S}$  and  $\delta^{33}\text{S}$  relationship (Farquhar et al., 2003; Johnston et al., 2005a; Pellerin et al., 2015). Comparative physiological studies have shown that BSD can produce  $^{33}\text{S}$ - $^{32}\text{S}$  fractionations between sulfate and sulfide that are slightly greater than those for MSR, when normalized to the same degree of  $^{34}\text{S}$ - $^{32}\text{S}$  fractionation (Johnston et al., 2005a). As a result,  $^{33}\text{S}$  enrichments in Mesoproterozoic carbonate-associated sulfate have been interpreted as a signal of active BSD (Johnston et al., 2005b). However, the large fractionations of  $^{34}\text{S}$ ,  $^{33}\text{S}$ , and  $^{32}\text{S}$  during MSR at low cell-specific sulfate reduction rates can mimic the effects of BSD in the sulfate reservoir (Sim et al., 2011), necessitating an alternative approach to identify the imprint of BSD in ancient sedimentary rocks. Here we focus on stratigraphic variation in the isotopic composition of Neoproterozoic pyrites, and use a steady-state isotope model to investigate how intrinsic microbial fractionations are translated into pyrite S isotopes.

We measured  $\delta^{34}\text{S}$  and  $\Delta^{33}\text{S}$  in sedimentary pyrites within organic-rich shale intervals deposited at storm wave base from a ca. 835–630 Ma Neoproterozoic sedimentary succession in Svalbard (Fig. 1) to evaluate the global significance of BSD through this critical interval in Earth history ( $\Delta^{33}\text{S} = \delta^{33}\text{S} - 1000 \times [1 + (\delta^{34}\text{S}/1000)^{33\lambda_{\text{ref}}}] - 1$ ), where  $^{33}\lambda_{\text{ref}}$  is equal to 0.515 and approximates low-temperature equilibrium mass-dependent fractionation). Our conclusions are further bolstered by new data from the post-Marinoan of Australia and Canada, the ca. 1460 Ma Belt Supergroup of the United States, and published data from Paleoproterozoic and Mesoproterozoic sedimentary pyrites from Russia and Canada.

## RESULTS

The  $\delta^{34}\text{S}$  values show a gradual increase from  $-25.7\text{‰}$  in the uppermost Veteranen Group to  $+40.0\text{‰}$  in the post-Sturtian Arena Formation (Fig. 1). Following this maximum,  $\delta^{34}\text{S}$  values gradually decrease to  $-17.6\text{‰}$  below the Marinoan Wilsonbreen diamictite. The post-Marinoan  $\delta^{34}\text{S}$  record shows an overall increase from  $-26.9\text{‰}$  to  $+22.3\text{‰}$  with second-order variability.  $\Delta^{33}\text{S}$  values show some scatter in the pre-Sturtian units (Fig. 1) and reach their most negative value of  $-0.175\text{‰}$  in the post-Sturtian Arena Formation. The  $\Delta^{33}\text{S}$  values gradually increase during the Cryogenian, mirroring  $\delta^{34}\text{S}$ , which is characteristic of fractionations dominated by MSR (Farquhar et al., 2003). In contrast, an upsection trend to a maximum  $\Delta^{33}\text{S}$  value of  $+0.232\text{‰}$  parallels increasing  $\delta^{34}\text{S}$  values in the post-Marinoan Dracoiisen Formation with remarkably little scatter (Fig. 1). Following this maximum,  $\Delta^{33}\text{S}$  values gradually decrease at the top of the section.

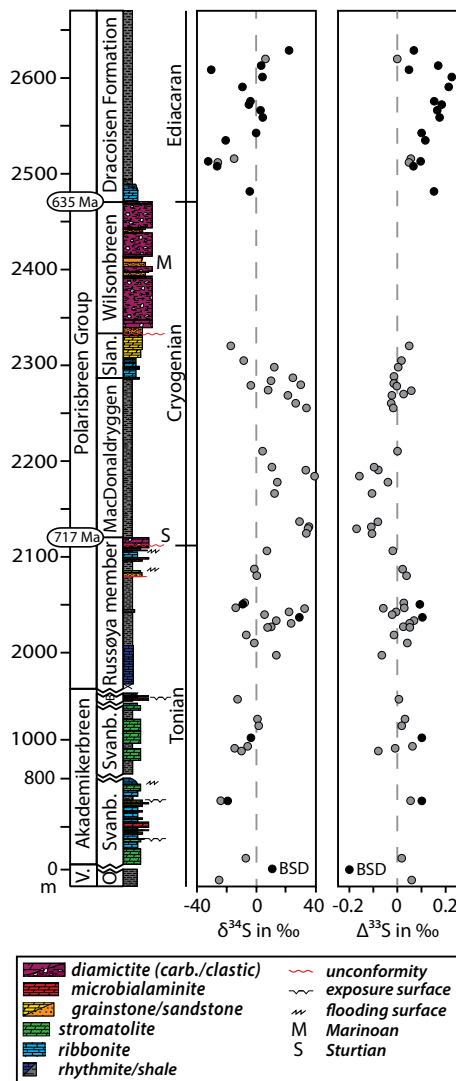


**Figure 1. Chemostratigraphy of the Neoproterozoic succession in Svalbard. Analytical error is smaller than symbol size. BSD—bacterial sulfur disproportionation. V.—Veteranen Group; O—Oxfordbreen Formation; Svanb.—Svanbergfjellet Formation; B—Backlundtoppen Formation; Slan.—Slangen Member.**

## DISCUSSION

We assume that our pyrites predominantly formed in pore waters because paleoredox data from these locations suggest deposition under oxic to anoxic-ferruginous conditions (Kunzmann et al., 2015; see the GSA Data Repository<sup>1</sup>). Therefore, we created a steady-state, isotope mass-balance model for pyrite formed in pore waters based on a published model (Berner, 1964) for net pore-water sulfate consumption, defined here as the difference between the sulfate consumed during MSR and that produced during

<sup>1</sup>GSA Data Repository item 2017054, additional information, methods, and data, is available online at [www.geosociety.org/datarepository/2017](http://www.geosociety.org/datarepository/2017), or on request from [editing@geosociety.org](mailto:editing@geosociety.org).

BSD. Our model assumes that the isotopic composition of pyrite tracks the isotopic composition of aqueous sulfide produced during net sulfate consumption, and that the aqueous sulfide produced is trapped essentially instantaneously as pyrite. By considering isotopic fractionation during net sulfate consumption, our model calculations can distinguish the isotopic influences of MSR and BSD (Pellerin et al., 2015; Fig. 2). In our first model runs, we set the net fractionation factors for pyrite production,  $^{33}\lambda_{\text{net}}$  to 0.513 and  $^{34}\alpha_{\text{net}}$  to 0.95 (Fig. 2A); these are both reasonable values for a population of sulfate reducing microbes (Johnston et al., 2005a). With these fractionations, our model reproduces more than 90% of pre-Marinoan Neoproterozoic pyrite data via MSR alone when the sulfate in the overlying seawater is set to vary between  $-0.1\text{‰}$  and  $-0.2\text{‰}$  for  $\Delta^{33}\text{S}$  and between  $10\text{‰}$  and  $40\text{‰}$  for  $\delta^{34}\text{S}$  (Fig. 2A). Such  $\delta^{34}\text{S}$  variation is consistent with the strong isotopic and concentration fluctuations that have been inferred for the Neoproterozoic seawater sulfate reservoir (Hurtgen et al., 2005). The variation in  $\Delta^{33}\text{S}$  in our model is consistent with the negative  $\Delta^{33}\text{S}$  values that have been estimated for early- and mid-Proterozoic seawater sulfate (Johnston et al., 2008; Scott et al., 2014). Thus we conclude that reoxidative S cycling was at most a local phenomenon in Svalbard sediments deposited before the Marinoan glaciation.

The trend of steeply increasing  $\Delta^{33}\text{S}$  values with increasing  $\delta^{34}\text{S}$  values in sedimentary pyrites from the post-Marinoan Dracoiisen Formation, however, cannot be reproduced by a model with isotopic fractionation imposed only by MSR, even if the sulfate isotope composition of overlying seawater is taken to have positive  $\delta^{34}\text{S}$  and  $\Delta^{33}\text{S}$  values (Fig. 2B), as recently determined for the immediate post-Marinoan sulfate reservoir (Crockford et al., 2016). This trend can only be reproduced by increasing  $^{33}\lambda_{\text{net}}$  to 0.516 (Fig. 2C), which is well above the limit for MSR (Farquhar et al., 2003; Johnston et al., 2005a; Sim et al., 2011) and requires significant disproportionation of intermediate S compounds (>80% of all sulfide produced by MSR is reoxidized; see the Data Repository) in concert with relatively intense MSR (Pellerin et al., 2015). Therefore, our results suggest significant reoxidative S cycling in Svalbard sediments in the aftermath of the ca. 635 Ma Marinoan glaciation.

To test the potential global nature of Ediacaran reoxidative S cycling, we measured pyrite S isotopes from post-Marinoan shales of the lower part of the early Ediacaran Sheepbed Formation (younger than 635 Ma) in northwestern Canada and from the latest Cryogenian–earliest Ediacaran upper Black River Dolomite in Tasmania ( $640.7 \pm 5.7$  Ma) (Kendall et al., 2009; Rooney et al., 2014). These data plot in the field of disproportionation (Fig. 2D). Thus, it seems that the significant reoxidative S cycling seen in

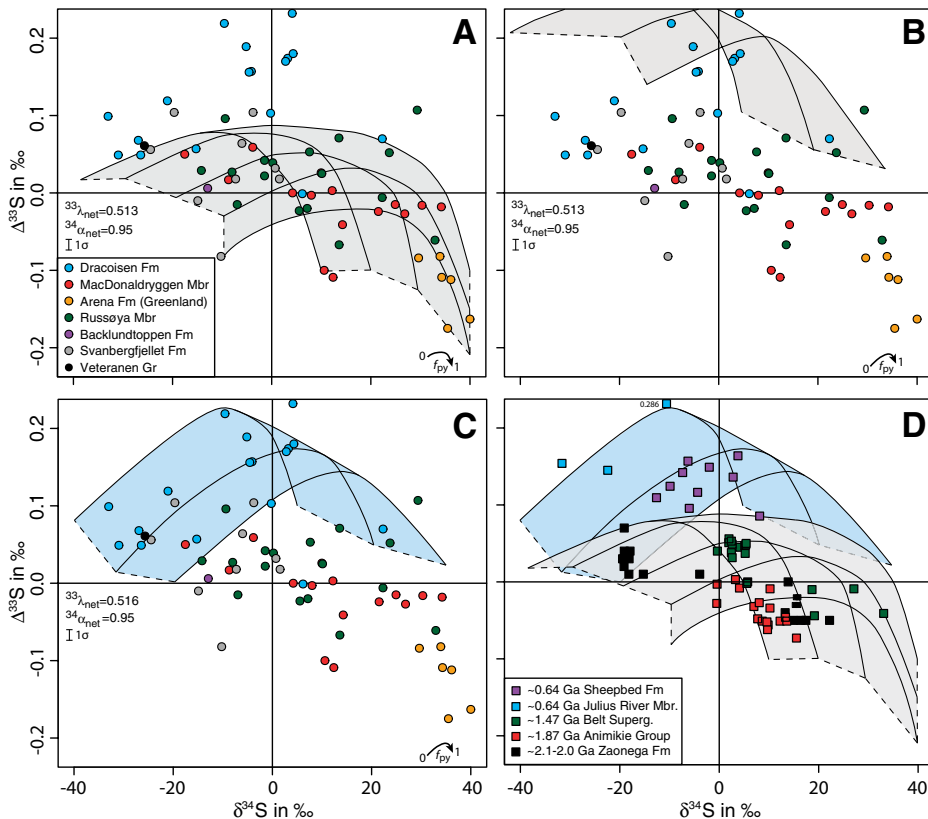


**Figure 2. Measured, modeled, and compiled  $\delta^{34}\text{S}$  and  $\Delta^{33}\text{S}$  data. A: Individual curves represent modeled pyrite isotopic compositions formed from a sulfate pool with an isotopic composition at the right end of the curve; pyrites evolve along curves from left to right with sulfate consumption. More than 90% of pre-Marinoan samples plot in the model field for pyrites formed by microbial sulfate reduction (MSR) only. A few samples from the pre-Marinoan Russoya Member (Mbr) and Svanbergfjellet Formation, as well as samples from the post-Marinoan Dracoisen Formation, require bacterial sulfur disproportionation (BSD). Gr—group. B: MSR-only models fail to reproduce the data from the post-Marinoan Dracoisen Formation even when the starting composition of sulfate is set to positive  $\delta^{34}\text{S}$  and  $\Delta^{33}\text{S}$  values. C: The model field can span the data from the post-Marinoan Dracoisen Formation with a single change in the model: increasing  $^{33}\lambda_{\text{net}}$  (which reflects the intensity of isotopic preference for  $^{33}\text{S}$  during net sulfate consumption) from 0.513 to 0.516, a value requiring BSD. D: Compilation of literature data and additional analysis. Published data are from Scott et al. (2014) (Zaonega) and Johnston et al. (2006) (Animikie). The reproducibility ( $1\sigma$ ) of analyses (replicate samples) is estimated to be better than 0.1‰ for  $\delta^{34}\text{S}$  and 0.015‰ for  $\Delta^{33}\text{S}$ . Superg—supergroup.**

the early Ediacaran of Svalbard was widespread and likely global in nature, starting immediately after the Marinoan glacial interval and lasting for at least the duration over which our samples were deposited (~5 m.y.). Sedimentary rocks from the ca. 580 Ma Buah Formation in Oman were independently interpreted to reflect BSD (Wu et al., 2015), suggesting that reoxidative S cycling was a persistent part of the sulfur cycle throughout the Ediacaran, even though the Ediacaran ocean may have been dominantly anoxic (Sperling et al., 2015; Sahoo et al., 2016).

In order to evaluate whether a globally significant reoxidative S cycle operated before the earliest Ediacaran, we compiled previously published  $\delta^{34}\text{S}$  and  $\Delta^{33}\text{S}$  data from Paleoproterozoic pyrites. Like our samples from Svalbard, all shales were deposited under ferruginous conditions (Fig. DR3). Together with new measurements from the ca. 1460 Ma Belt Supergroup, this compilation

demonstrates that S isotope data in Paleoproterozoic and Mesoproterozoic pyrites do not require BSD (Fig. 2D). The lack of a globally operating reoxidative S cycle throughout most of the Proterozoic indicates qualitatively an increase in atmospheric  $\text{O}_2$  in the earliest Ediacaran. This result does not preclude transient fluctuations in oxygen levels earlier in the Proterozoic (Bachan and Kump, 2015). The exact timing of the earliest Ediacaran oxygenation appears to be coincident with the end of the Marinoan glacial interval. This testable prediction can be evaluated in the future from ferruginous pre-Marinoan strata in the Canadian and Australian basins studied here (Fig. 2D). Although the timing of this oxidative onset may suggest a causal link between increasing atmospheric  $\text{O}_2$  levels and animal diversification and marine ecosystem complexity, calibration of the oxygen demand of BSD is needed to make this possible link quantitative.

Sulfate levels in the immediate aftermath of the Marinoan glaciation may have been as low as  $<300 \mu\text{M}$  (Crockford et al., 2016) and perhaps rose to near modern levels ( $>17 \text{ mM}$ ; Horita et al., 2002) at the Precambrian-Cambrian boundary. With due recognition of the significant uncertainties associated with these estimates, the Ediacaran likely underwent a first-order increase in marine sulfate concentrations. Ediacaran bioturbation has been proposed as a driver for this rise (Canfield and Farquhar, 2009), but sedimentary fabrics indicate that animals did not begin to thoroughly mix sediments until the late Silurian (Tarhan et al., 2015). Enhanced microbial sulfide oxidation followed by BSD at or near the sediment-seawater interface (Canfield and Teske, 1996), however, will inevitably increase seawater sulfate levels by reducing the amount of sulfur buried as pyrite. Relative oxidative S fluxes as inferred from the Svalbard samples ( $>80\%$  of all sulfide produced by MSR oxidized; see the Data Repository) can sustain marine sulfate concentrations that are at least 5 and perhaps 100 times greater than what would be possible without reoxidative S cycling (see the Data Repository), providing a plausible mechanism for elevated seawater sulfate in the absence of bioturbation. The first-order increase of the Ediacaran sulfate reservoir may have ultimately ushered in a Phanerozoic-style sulfur cycle.

#### ACKNOWLEDGMENTS

We thank Itay Halevy, Ulrich Wortmann, André Pellerin, and Erik Sperling for discussions, and Lee Kump, Huiming Bao, Dave Johnston, and three anonymous reviewers for insightful comments. Wing acknowledges funding from the Natural Sciences and Engineering Research Council of Canada and the Fonds de Recherche du Québec—Nature et Technologies (FRQNT). Halverson acknowledges funding by the U.S. National Science Foundation (NSF) and the American Chemical Society. Lyons acknowledges funding by the NASA Astrobiology Institute and the NSF ELT (Earth-Life Transitions) Program. Kunzmann publishes with permission of the executive director of the Northern Territory Geological Survey.

#### REFERENCES CITED

- Aller, R.C., and Rude, P.D., 1988, Complete oxidation of solid phase sulfides by manganese and bacteria in anoxic marine sediments: *Geochimica et Cosmochimica Acta*, v. 52, p. 751–765, doi:10.1016/0016-7037(88)90335-3.
- Bachan, A., and Kump, L.R., 2015, The rise of oxygen and siderite oxidation during the Lomagundi Event: *National Academy of Sciences Proceedings*, v. 112, p. 6562–6567, doi:10.1073/pnas.1422319112.
- Berner, R.A., 1964, An idealized model of dissolved sulfate distribution in recent sediments: *Geochimica et Cosmochimica Acta*, v. 28, p. 1497–1503, doi:10.1016/0016-7037(64)90164-4.
- Blamey, N.J.F., Brand, U., Parnell, J., Spear, N., Lécuyer, C., Benison, K., Meng, F., and Ni, P., 2016, Paradigm shift in determining Neoproterozoic atmospheric oxygen: *Geology*, v. 44, p. 651–654, doi:10.1130/G37937.1.
- Canfield, D.E., and Farquhar, J., 2009, Animal evolution, bioturbation, and the sulfate concentration

- of the oceans: National Academy of Sciences Proceedings, v. 106, p. 8123–8127, doi:10.1073/pnas.0902037106.
- Canfield, D.E., and Teske, A., 1996, Late Proterozoic rise in atmospheric oxygen concentration inferred from phylogenetic and sulfur isotope studies: *Nature*, v. 382, p. 127–132, doi:10.1038/382127a0.
- Canfield, D.E., Thamdrup, B., and Fleischer, S., 1998, Isotope fractionation and sulfur metabolism by pure and enrichment cultures of elemental sulfur-disproportionating bacteria: *Limnology and Oceanography*, v. 43, p. 253–264, doi:10.4319/l.o.1998.43.2.0253.
- Canfield, D.E., Farquhar, J., and Zerkle, A.L., 2010, High isotope fractionations during sulfate reduction in a low-sulfate euxinic ocean analog: *Geology*, v. 38, p. 415–418, doi:10.1130/G30723.1.
- Crockford, P.W., et al., 2016, Triple oxygen and multiple sulfur isotope constraints on the evolution of the post-Marinoan sulfur cycle: *Earth and Planetary Science Letters*, v. 435, p. 74–83, doi:10.1016/j.epsl.2015.12.017.
- Elsgaard, L., and Jørgensen, B.B., 1992, Anoxic transformations of radiolabeled hydrogen sulfide in marine and freshwater sediments: *Geochimica et Cosmochimica Acta*, v. 56, p. 2425–2435, doi:10.1016/0016-7037(92)90199-S.
- Farquhar, J., Johnston, D.T., Wing, B.A., Habicht, K.S., Canfield, D.E., Airieau, S., and Thiemens, M.H., 2003, Multiple sulphur isotopic interpretations of biosynthetic pathways: Implications for biological signatures in the sulphur isotope record: *Geobiology*, v. 1, p. 27–36, doi:10.1046/j.1472-4669.2003.00007.x.
- Horita, J., Zimmermann, H., and Holland, H.D., 2002, Chemical evolution of seawater during the Phanerozoic: Implications from the record of marine evaporites: *Geochimica et Cosmochimica Acta*, v. 66, p. 3733–3756, doi:10.1016/S0016-7037(01)00884-5.
- Hurtgen, M.T., Arthur, M.A., and Halverson, G.P., 2005, Neoproterozoic sulfur isotopes, the evolution of microbial sulfur species, and the burial efficiency of sulfide as sedimentary pyrite: *Geology*, v. 33, p. 41–44, doi:10.1130/G20923.1.
- Johnston, D.T., Farquhar, J., Wing, B.A., Kaufman, A.J., Canfield, D.E., and Habicht, K.S., 2005a, Multiple sulfur isotope fractionations in biological systems: A case study with sulfate reducers and sulfur disproportionators: *American Journal of Science*, v. 305, p. 645–660, doi:10.2475/ajs.305.6-8.645.
- Johnston, D.T., Wing, B.A., Farquhar, J., Kaufman, A.J., Strauss, H., Lyons, T.W., Kah, L.C., and Canfield, D.E., 2005b, Active microbial sulfur disproportionation in the Mesoproterozoic: *Science*, v. 310, p. 1477–1479, doi:10.1126/science.1117824.
- Johnston, D.T., Poulton, S.W., Fralick, P.W., Wing, B.A., Canfield, D.E., and Farquhar, J., 2006, Evolution of the oceanic sulfur cycle at the end of the Paleoproterozoic: *Geochimica et Cosmochimica Acta*, v. 70, p. 5723–5739, doi:10.1016/j.gca.2006.08.001.
- Johnston, D.T., Farquhar, J., Summons, R.E., Shen, Y., Kaufman, A.J., Masterson, A.L., and Canfield, D.E., 2008, Sulfur isotope biogeochemistry of the Proterozoic McArthur basin: *Geochimica et Cosmochimica Acta*, v. 72, p. 4278–4290, doi:10.1016/j.gca.2008.06.004.
- Jørgensen, B.B., 1990, A thiosulfate shunt in the sulfur cycle of marine sediments: *Science*, v. 249, no. 4965, p. 152–154, doi:10.1126/science.249.4965.152.
- Kendall, B., Creaser, R.A., Calver, C.R., Raub, T.D., and Evans, D.A.D., 2009, Correlation of Sturtian diamictite successions in southern Australia and northwestern Tasmania by Re-Os black shale geochronology and the ambiguity of “Sturtian”-type diamictite-cap carbonate pairs as chronostratigraphic marker horizons: *Precambrian Research*, v. 172, p. 301–310, doi:10.1016/j.precamres.2009.05.001.
- Kunzmann, M., Halverson, G.P., Scott, C.T., Minarik, W.G., and Wing, B.A., 2015, Geochemistry of Neoproterozoic black shales from Svalbard: Implications for oceanic redox conditions spanning Cryogenian glaciations: *Chemical Geology*, v. 417, p. 383–393, doi:10.1016/j.chemgeo.2015.10.022.
- Pellerin, A., Bui, T.H., Rough, M., Mucci, A., Canfield, D.E., and Wing, B.A., 2015, Mass-dependent sulfur isotope fractionation during reoxidative sulfur cycling: A case study from Mangrove Lake, Bermuda: *Geochimica et Cosmochimica Acta*, v. 149, p. 152–164, doi:10.1016/j.gca.2014.11.007.
- Rooney, A.D., Macdonald, F., Strauss, J.V., Dudás, F.Ö., Hallmann, C., and Selby, D., 2014, Re-Os geochronology and coupled Os-Sr isotope constraints on the Sturtian snowball Earth: *National Academy of Sciences Proceedings*, v. 111, p. 51–56, doi:10.1073/pnas.1317266110.
- Sahoo, S.K., Planavsky, N.J., Jiang, G., Kendall, B., Owens, J.D., Wang, X., Shi, X., Anbar, A.D., and Lyons, T.W., 2016, Oceanic oxygenation events in the anoxic Ediacaran ocean: *Geobiology*, v. 14, p. 457–468, doi:10.1111/gbi.12182.
- Schippers, A., and Jørgensen, B.B., 2001, Oxidation of pyrite and iron sulfide by manganese dioxide in marine sediments: *Geochimica et Cosmochimica Acta*, v. 65, p. 915–922, doi:10.1016/S0016-7037(00)00589-5.
- Schippers, A., and Jørgensen, B.B., 2002, Biogeochemistry of pyrite and iron sulfide oxidation in marine sediments: *Geochimica et Cosmochimica Acta*, v. 66, p. 85–92, doi:10.1016/S0016-7037(01)00745-1.
- Scott, C.T., Wing, B.A., Bekker, A., Planavsky, N.J., Medvedev, P., Bates, S.M., Yun, M., and Lyons, T.W., 2014, Pyrite multiple-sulfur isotope evidence for rapid expansion and contraction of the early Paleoproterozoic seawater sulfate reservoir: *Earth and Planetary Science Letters*, v. 389, p. 95–104, doi:10.1016/j.epsl.2013.12.010.
- Sim, M.S., Bosak, T., and Ono, S., 2011, Large sulfur isotope fractionation does not require disproportionation: *Science*, v. 333, p. 74–77, doi:10.1126/science.1205103.
- Sperling, E.A., Wolock, C.J., Morgan, A.S., Gill, B.C., Kunzmann, M., Halverson, G.P., Macdonald, F.A., Knoll, A.H., and Johnston, D.T., 2015, Statistical analysis of iron geochemical data suggests limited late Proterozoic oxygenation: *Nature*, v. 523, p. 451–454, doi:10.1038/nature14589.
- Tarhan, L.G., Droser, M.L., Planavsky, N.J., and Johnston, D.T., 2015, Protracted development of bioturbation through the early Palaeozoic Era: *Nature Geoscience*, v. 8, p. 865–869, doi:10.1038/ngeo2537.
- Thamdrup, B., Finster, K., Würgler Hanson, J., and Bak, F., 1993, Bacterial disproportionation of elemental sulfur coupled chemical reduction of iron or manganese: *Applied and Environmental Microbiology*, v. 59, p. 101–108.
- Wing, B.A., and Halesy, I., 2014, Intracellular metabolite levels shape sulfur isotope fractionation during microbial sulfate respiration: *National Academy of Sciences Proceedings*, v. 111, p. 18116–18125, doi:10.1073/pnas.1407502111.
- Wu, N., Farquhar, J., and Fike, D.A., 2015, Ediacaran sulfur cycle: Insights from sulfur isotope measurements ( $\Delta^{33}\text{S}$  and  $\delta^{34}\text{S}$ ) on paired sulfate-pyrite in the Huqf Supergroup of Oman: *Geochimica et Cosmochimica Acta*, v. 164, p. 352–364, doi:10.1016/j.gca.2015.05.031.

Manuscript received 14 September 2016  
 Revised manuscript received 13 November 2016  
 Manuscript accepted 14 November 2016

Printed in USA